

## Reaction-Induced Phase Separation Dynamics: A Polymer in a Liquid Crystal Solvent

J. B. Nephew, T. C. Nihei, and S. A. Carter\*

*Physics Department, University of California, Santa Cruz, California 95064*

(Received 8 September 1997)

The dynamics of addition polymerization-induced phase separation in a liquid crystal solvent is examined via confocal microscopy in systems where the final morphology consists of nematic liquid crystal domains suspended in a cross-linked polymer matrix. For low polymer concentrations, we observe unusually rapid hydrodynamics and coalescence during phase separation that determine the final composite morphology. This hypercoalescence can result from polymerization-induced changes of the solubility of the polymer matrix in the liquid crystal solvent. [S0031-9007(98)05859-1]

PACS numbers: 61.30.-v, 61.41.+e, 64.75.+g

Phase separation dynamics of a mixture thermally quenched from a stable to unstable regime in the phase diagram has been extensively studied in alloys, binary fluids, and polymer mixtures [1]. Alloys and binary fluids can be reasonably explained by conventional theories of Cahn-Hilliard [2] or the Hohenberg-Halperin notation [3], where the interfacial tension plays a major role in determining the morphology. For thermally quenched polymer mixtures, Takana has shown that dynamic asymmetry can result from the slow kinetics associated with the polymer glass transition, and that in this case the domain shape is determined by the mechanical balance of elastic forces, resulting in spongelike continuous patterns of the *minority* polymer phase to form [4]. For reaction-induced phase separation in binary polymer mixtures, Tran-Cong and Harada have demonstrated that a variety of mesoscopic structures can form with elastic stress playing an important role in the morphology when the reacting polymer is a minority phase [5].

An interesting variant of this problem has been to understand phase separation kinetics when the polymer is diluted in an anisotropic solvent, such as liquid crystals. Here, one has three competing dynamics: one dominated by the transition from isotropic to nematic ordering of the liquid crystal, a second determined by the phase separation of the polymer from the liquid crystal solvent where the anisotropy of the solvent can affect solubility, and a third determined by the growing molecular weight and gelation of the polymer matrix [6]. Recently, Boots *et al.* have shown that elastic forces in the polymer matrix also play a role in determining the morphology in polymer dispersed liquid crystal (PDLC) systems [7].

In this Letter, we use time resolved confocal microscopy at high resolution (200 nm) and high speed (100 ms) to study the reaction-induced phase transition kinetics in polymer(monomer)/liquid crystal mixtures very near the initial phase separation. We observe unusual hydrodynamics and coalescence which are not explained by current theories of reaction-induced phase separation but dramatically affect the final morphology. We determine the kinetic phase separation diagram for a spongelike polymer/liquid crystal composite and demonstrate that this phase dia-

gram can be extended to other systems, allowing us to predict the temperature and composition dependence of the final morphology in dropletlike PDLC systems also. Finally, we observe a crossover from elastic to the hypercoalescence dominated regimes via the dilution of the monomer/polymer.

The monomer used in this work, Merck PN393 (2-ethyl hexyl acrylate monomer and trimethylol propane triacrylate cross-linker), and the liquid crystal Merck TL213 (halogenated biphenyl), were chosen because they have been well studied and are known to form a spongelike morphology at low monomer concentrations upon irradiation. The critical concentration range for spongelike morphology is 27% to 18% monomer by volume [8,9]. The dynamics are similar over this range; we concentrated our studies on 20% monomer solutions. For comparison, we also studied a mixture of the monomer Norland Optical Adhesive 65 (NOA65—trimethylolpropane diallyl ether, trimethylolpropane trithiol, and isophorone diisocyanate ester) and the liquid crystal Merck E7 (cyanobiphenyl compounds), which results in a droplet morphology over a large composition range of monomer from 20% to 60% [10]. The mixture of monomer and nematic liquid crystals results in an isotropic solution at room temperature prior to photopolymerization. A fluorescent dichroic dye, Exciton pyrromethane 580, was used to increase contrast between the polymer and the liquid crystal. The temperature range was bounded by the isotropic-nematic transition near 15 °C and the lack of a visible phase separation on full polymerization near 70 °C. The phase diagrams for the PN393/TL213 and NOA65/E7 mixtures have been reported elsewhere [8,10]. We used both 10 and 25  $\mu\text{m}$  gap cells to show that the phase separation dynamics does not depend on surface interactions with the cells prepared as described previously [9]. A Nikon-2 Optiphot microscope, Technical Instrument's confocal attachment, and a 1.4 NA 100 $\times$  oil-emersion lens yielded an effective resolution of 200 nm horizontal and 400 nm vertical. The Hg lamp on the microscope with an estimated power output of 10 mW/cm<sup>2</sup> at 365 nm was used to initiate the free radical polymerization over a limited area (200  $\mu\text{m}$   $\times$  200  $\mu\text{m}$ ); this unique geometry allowed

us to take several measurements on the same cell, polymerize uniformly, relieve contraction-induced stress [5], and take data simultaneous with the polymerization [11]. The phase separation "movie" consisted of over 40 digital images which were taken with a 12-bit Xillex Micro-imager camera.

In Fig. 1, we show the time resolved morphologies of the PN393/TL213 polymer liquid crystal mixture at 20% polymer concentration and at low (21 °C) and high (38 °C) temperatures, where the frames are limited to six each for space considerations. In frame 1, we first observe the nucleation of the nematic liquid crystal domains caused by the increase in the liquid crystalline molecule nearest neighbors as the monomers react to form polymers. As the addition polymerization reaction continues, nematic domains continue to nucleate but are mainly static, i.e., they do not move or grow in size via Oswald ripening or molecular diffusion, until fast movement followed by very rapid coalescence starts to be observed in frame 3. To our knowledge, coalescence of this nature has not been previously observed in PDLCs; this could be due to the small size scale and short time scale for which these dynamics exist. The fast kinetics occurs for a few seconds after which the hypercoalescence ceases, because the polymer matrix has either grown sufficiently in molecular weight or reached its gel point, impeding further coalescence. Next, the polymer and remaining solution continue to expel liquid crystal, causing the nematic domains to grow in radius for several seconds, until visible changes in the matrix are suppressed, and longer-term elastic effects are expected to dominate. The resulting morphology consists of liquid crystal domains dispersed in a spongelike polymer matrix with the domain size increasing with increasing UV cure temperature.

These dynamics are unique to the polymerization-induced phase separation; thermally quenching the sample below its diluted isotropic-nematic phase transition ( $T \sim 15^\circ\text{C}$ ) results in domain growth primarily by nucleation and growth, Oswald ripening, and molecular diffusion, in agreement with standard theories of phase separation in binary fluids [1]. Free radical polymerization at high temperatures ( $T \sim 70^\circ\text{C}$ ), above the pure liquid crystal isotropic-nematic transition, results in zero effective cross linking; subsequent heating and cooling through this transition causes the polymer matrix to undergo a swelling/deswelling transition, with no hypercoalescence and subsequent minor changes in final morphology. These results are consistent with the polymer acting as a microgel [12].

We summarize our results using three time scales:  $t_n$ , the time it takes for the nematic domains to grow to an observable size (representative of the LC isotropic-nematic phase transition);  $t_c$  the time when the hypercoalescence is initiated; and  $t_g$ , the time for the polymer matrix to sufficiently solidify or gel such that elastic effects dominate. The temperature dependence of  $t_n$  (circles),  $t_c$  (squares), and  $t_g$  (triangles) at  $15 < T < 45^\circ\text{C}$  is summarized in

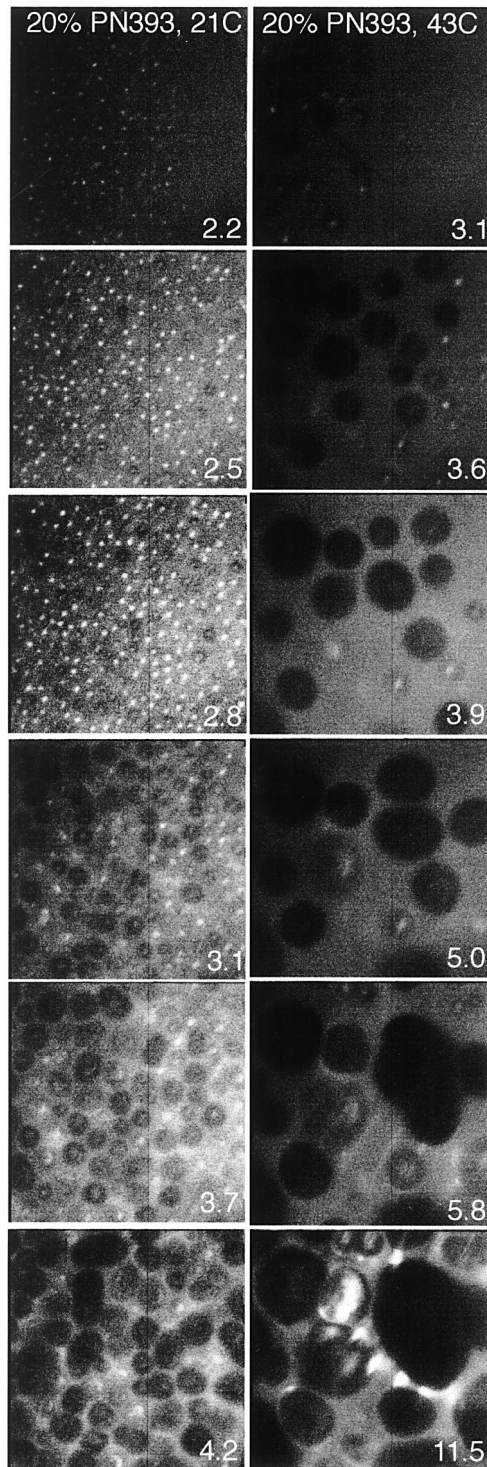


FIG. 1. 20% PN393 monomer mixed with liquid crystal TL213 polymerized at 21 °C (left side) and 38 °C (right side) showing the rapid coalescence and hydrodynamics. Above 4.0 and 6.0 sec, respectively, coalescence is no longer observed. Images are  $13.8 \times 13.8 \mu\text{m}$ .

Fig. 2 for the TL213/PN393 system. The transition time for the isotropic-nematic transition  $t_n$  increases with increasing temperature as the distance from the phase boundary line increases [8]. The fast kinetics and hypercoalescence time  $t_c$  are temperature independent. This

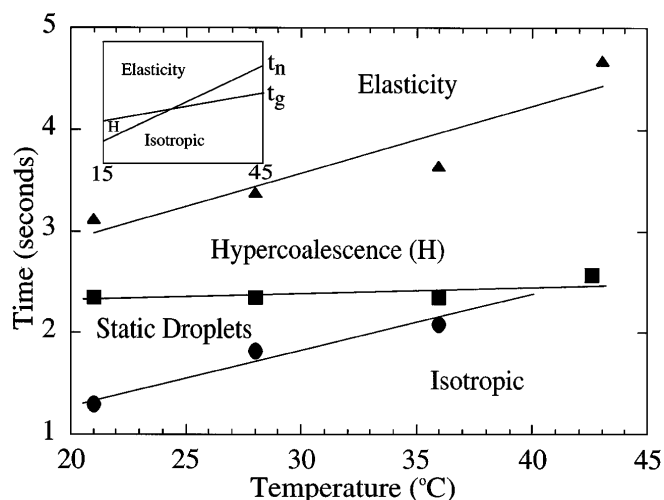


FIG. 2. Time after free radical initiation versus cure temperature diagram for PN393/TL213 mixture (main) and NOA65/E7 mixture (inset). The different regimes are explained in text. Lines are guides to the eye.

result combined with studies at different polymerization rates indicate that  $t_c$  depends on the extent of polymerization and not on the fraction of nematic liquid crystal that has phase separated which is strongly temperature dependent. Finally, we observe that the solidification or gel time increases with increasing temperature, as does the difference  $t_g - t_c$ , allowing for longer hypercoalescence times and, therefore, explaining the larger final domains observed. The increase in the solidification time is due to the increase in the solubility of the LC in the monomer as temperature increases [12].

Phase separations explained by the usual thermodynamic arguments based on the extent of the polymer matrix at the isotropic-nematic phase transition would expect smaller domains at higher temperature, as is found for the well-studied E7/NOA65 system [6,7,10]. For comparison, we repeated these experiments on the E7/NOA65 system which allowed us to achieve monomer concentrations as high as 60% by volume. At room temperature, the E7 liquid crystal phase separated from the NOA65 monomer at 20% monomer concentration; therefore, the cell was heated to 35 °C in order to get a homogeneous solution at 20% for direct comparison to the TL213/PN393 systems. We observe the same dynamics and phase diagram as before, with the E7 forming a more “dropletlike” morphology. These dynamics are shown on the left side of Fig. 3. If the monomer concentration is increased to 40%, then these dynamics cease to occur, right side of Fig. 3, and we recover the results and morphology observed previously [7]. The phase diagram for the 40% E7/NOA65 system is shown in the inset of Fig. 2; it is qualitatively the same as in the main figure, but with a lowering of  $t_g$  with respect to  $t_n$ , which results in the solidification point occurring before the nucleation of the nematic domains ( $t_g < t_n$ );  $t_g$  is effectively lowered due to the increase in monomer concentration [12]. For  $t_g < t_n$ , elastic effects domi-

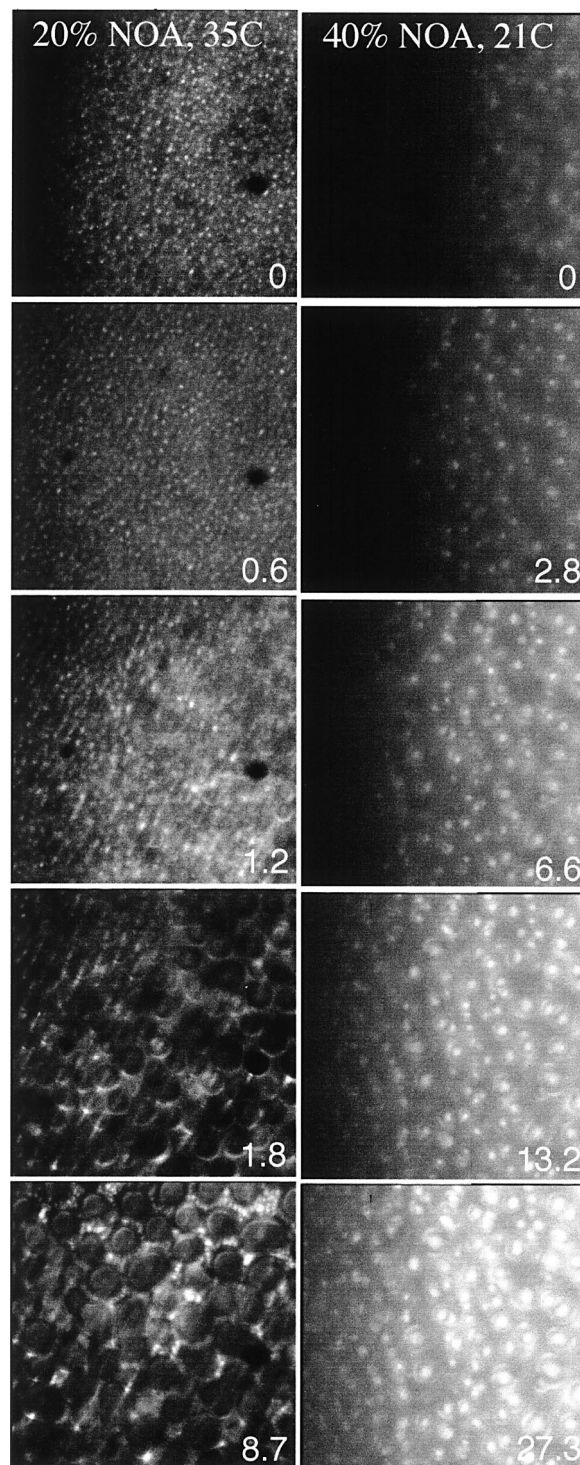


FIG. 3. Mixtures of liquid crystal E7 with 20% NOA65 monomer polymerized at 35 °C (left side) and 40% NOA65 monomer polymerized at 21 °C (right side). The rapid coalescence is observed only for low monomer concentrations. Images are  $13.8 \times 13.8 \mu\text{m}$ .

nate as recently shown by the Phillips group [7], and no hypercoalescence is observed. In all systems studied, the initial nucleation regime ( $t_c > t > t_n$ ) is characterized by a quasiperiodic spatial appearance of nematic domains and the lack of any significant movement or growth of domains.

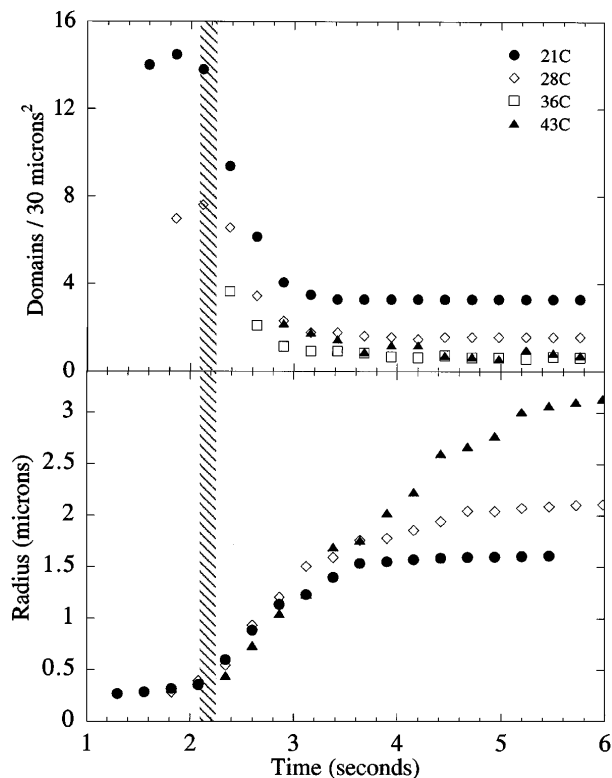


FIG. 4. Number of liquid crystal domains,  $n_{1c}$ , normalized to  $10 \mu\text{m}^2$  unit area (top) and average domain diameter  $d_{\text{avg}}$  (bottom) plotted versus time after initial polymerization.

To elucidate the mechanism for the hypercoalescence, we graph in Fig. 4 the number of nematic  $n_{1c}$  and the average diameter of the nematic domains  $d_{\text{avg}}$  as a function of time and varying UV cure temperatures. The time at which the rapid motion is initiated is clearly indicated in  $n_{1c}$ . The number of domains increases rapidly at early times for  $t > t_n$  as the nematic domains nucleate, falls off rapidly for  $t_c < t < t_g$  during the coalescence, and then finally stabilizes for  $t > t_g$ . The domain diameter  $d_{\text{avg}}$  is independent of cure temperature for  $t < t_c$ , is governed by the hypercoalescence for  $t_c < t < t_g$ , and is governed by the molecular diffusion for  $t > t_g$ . The changes  $d_{\text{avg}}$  and  $n_{1c}$  are clearly determined by a universal time scale rather than a temperature scale, indicating the phase separation kinetics is not governed so much by the phase transition of the liquid crystal from isotropic to nematic, which is strongly temperature dependent, but more by reaction-induced changes in the polymer matrix, which are strongly time dependent. The kinetics is also not affected by a  $10\times$  decrease in the polymerization rate. We speculate then that the mechanism for the hypercoalescence is caused by the polymer matrix collapsing, or becoming self-attractive, at a critical molecular weight which is determined by the solubility of the polymer matrix in the fluid solvent [12,13]. The data indicate that this solubility must be determined primarily by the molecular weight of the polymer; however, we note that the polymer is more soluble in an isotropic than anisotropic (nematic) solvent.

Several recent theoretical models and simulations have been undertaken to explain the kinetics of polymerization-induced phase separation in polymer-liquid crystal mixtures [14]. In general, the models consider only linear polymers or interactions between liquid crystals and/or surfaces which cannot account for the kinetics observed in the cross-linked polymer systems. Our studies also show that increasing the surface-induced shrinkage stress on the system or decreasing the effective cross-linking can cause the sponge and dropletlike morphologies to become unstable, with bicontinuous liquid crystal labyrinth patterns forming over long-time scales [4,15]. More simulations on cross-linked polymers and experiments on both linear and cross-linked polymers are needed to understand the richness of phase transitions and pattern formation in polymer/liquid crystal mixtures.

We thank K. Amundson and P. Drzaic for stimulating discussions. S.A.C. acknowledges support from the Packard Foundation; and J.B.N. and T.C.N. acknowledge support from the NSF REU program.

\*Corresponding author.

Electronic address: sacarter@cats.ucsc.edu

- [1] See, *Phase Transition and Critical Phenomena*, edited by C. Domb and J.L. Lebowitz (Academic Press, London, 1983); K. Binder, *Adv. Polym. Sci.* **112**, 181 (1994).
- [2] J. W. Cahn, *J. Chem. Phys.* **42**, 93 (1965).
- [3] P. C. Hohenberg and B. I. Halperin, *Rev. Mod. Phys.* **49**, 435 (1976); E. D. Siggia, *Phys. Rev. A* **20**, 595 (1979).
- [4] H. Takana, *J. Chem. Phys.* **100**, 5323 (1994), and references therein.
- [5] Qui Tran-Cong and Asuka Harada, *Phys. Rev. Lett.* **76**, 1162 (1996).
- [6] P. S. Drzaic, *Liquid Crystal Dispersions* (World Scientific, Singapore, 1995).
- [7] C. Serbutoviez *et al.*, *Liq. Cryst.* **22**, 145 (1997); H. M. J. Boots *et al.*, *Macromolecules* **29**, 7683 (1996); C. Serbutoviez *et al.*, *Macromolecules* **29**, 7690 (1996).
- [8] K. Amundson, A. Van Blaaderen, and P. Wiltzius, *Phys. Rev. E* **55**, 1646 (1997).
- [9] S. A. Carter *et al.*, *J. Appl. Phys.* **81**, 5992 (1997); J. D. LeGrange *et al.*, *J. Appl. Phys.* **81**, 5984 (1997).
- [10] A. J. Lovinger, K. R. Amundson, and D. D. Davis, *Chem. Mater.* **6**, 1726 (1994).
- [11] We tested the cell with an external light source and in bright field mode to make sure that the final morphology did not depend on our imaging technique.
- [12] P. G. DeGennes, *Scaling Concepts in Polymer Physics* (Cornell University, Ithaca, 1979).
- [13] Other theories, such as collision induced collisions [H. Tanaka, *Phys. Rev. Lett.* **72**, 1702 (1994)], attractive forces between liquid crystal droplets, and temperature-induced convection have been tested and are unable to explain the observed dynamics.
- [14] A. J. Liu and G. H. Fredrickson, *Macromolecules* **29**, 8000 (1996); P. I. C. Teixeira and B. M. Mulder, *Phys. Rev. E* **53**, 1805 (1996); A. Matsuyama and T. Kato, *J. Chem. Phys.* **105**, 1654 (1996); W.-J. Chen and S.-H. Chen, *Phys. Rev. E* **52**, 4549 (1995).
- [15] T. Nihei, J. Nephew, and S. A. Carter (unpublished).